

EXPERIMENTAL DETERMINATION OF THE NEUTRON CHANNELING LENGTH IN A PLANAR WAVEGUIDE

S. V. Kozhevnikov^{a,b,*}, *V. K. Ignatovich*^{a,**}, *F. Ott*^{c,d}, *A. Rühm*^b, *J. Major*^b

^a *Frank Laboratory of Neutron Physics, Joint Institute for Nuclear Research
141980, Dubna, Moscow Region, Russia*

^b *Max-Planck-Institut für Intelligente Systeme (formerly Max-Planck-Institut für Metallforschung)
D-70569, Stuttgart, Germany*

^c *CEA, IRAMIS, Laboratoire Léon Brillouin
F-91191, Gif sur Yvette, France*

^d *CNRS, IRAMIS, Laboratoire Léon Brillouin
F-91191, Gif sur Yvette, France*

Received November 12, 2012

In neutron waveguides, the neutron wave is confined inside the guiding layer of the structure and can escape from the layer edge as a microbeam. The channeling within the guiding layer is accompanied by an exponential decay of the neutron wave function density inside the waveguide. Here, we report direct determination of the corresponding decay constant, termed the neutron channeling length. For this, we measured the microbeam intensity as a function of the length of a neutron absorbing layer of variable length placed onto the surface of a waveguide structure. Such planar neutron waveguides transform a conventional neutron beam into an extremely narrow but slightly divergent microbeam, which can be used for the investigation of nanostructures with submicron spatial resolution.

DOI: 10.7868/S0044451013100052

Neutron scattering is a powerful tool for the investigation of magnetic structures, polymers, and biological objects. But the information obtained about the investigated systems is averaged over the neutron beam width, which is usually of the order of 0.1 to 10 mm. For investigations of nanostructures with high spatial resolution, focusing devices (such as focusing crystal monochromators or focusing guides) have been developed, which can focus the neutron beam in one or two dimensions. However, these devices are restricted by their physical properties and manufacturing technologies and cannot produce the beam focus of less than 50 μm width [1]. Potential devices for the production of submicron neutron beams in one dimension are layered planar waveguides, which transform a conventional neutron beam into an extremely narrow ($< 1 \mu\text{m}$), although slightly divergent (0.1°) neu-

tron microbeam emerging from the edge of a waveguide [2–5].

The phenomenon of neutron channeling was observed experimentally in [6–10]. The authors of [9], as reported by Nikitenko [11], carried out the first measurements for the structure Cu(300 Å)/Ti(1500 Å)/Cu(1000 Å)/glass(5 mm) at the time-of-flight reflectometer REMUR in Dubna (Russia) in 2000. Four resonance modes were observed. As it was described by Nikitenko, the neutron channeling length was measured as a function of the neutron wavelength. Several widths of a fixed absorber band on the sample surface were used. Later, in 2002, the experiments on the neutron channeling length measurements were continued for another structure Cu(300 Å)/Ti(3000 Å)/Cu(1500 Å)/glass(5 mm) at the reflectometer ADAM in ILL (Grenoble, France) [11]. The intensity of the monochromatic neutron beam exiting from the sample edge was measured. Both experiments were done in the vertical sample plane geometry. Therefore, a set of several samples with different absorber lengths was used.

*E-mail: kozhevn@nf.jinr.ru

**E-mail: ignatovi@nf.jinr.ru

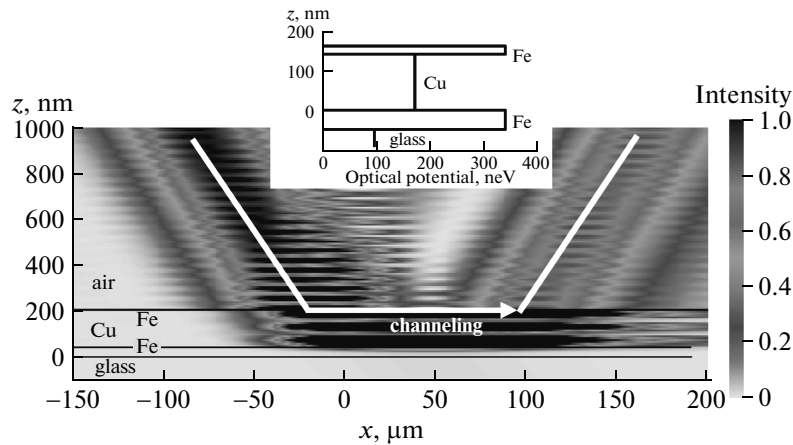


Fig. 1. Propagation of the neutron wave inside a Fe(10 nm)/Cu(150 nm)/Fe(50 nm) waveguide structure. The calculated neutron wave density as a function of the coordinate z perpendicular to the sample surface and the coordinate x along the beam propagation parallel to the sample surface. The neutron-optical potential inside the waveguide is presented in the inset

Our independent experiment [12,13] was carried out in 2010¹⁾. A horizontal sample plane geometry was used. We used a single sample to measure the channeling length for the resonance order $n = 0$. In this communication, we present a direct measurement of the channeling length and compare it with the theory [14]. We note that the case of neutrons is significantly different from the case of x-rays because the neutron absorption is very weak compared to the x-ray one. The absorption length of 4 Å neutrons in copper is 7.2 mm while it is 22 μm for 8 keV x-rays. The absorption is therefore not the main parameter defining the value of the channeling length, and this makes a direct measurement feasible.

The problem of neutron propagation at interfaces was already studied earlier. For example, we mention the attempts to measure the Goos–Hänchen (GH) effect at the total reflection of neutrons from a surface [15]. In the GH effect, the neutron propagates along the surface in the form of an evanescent wave. In the case of waveguides, it propagates in the form of resonant modes. In such a situation, the propagation length can be enhanced by several orders of magnitudes, making the measurement technically feasible.

¹⁾ Our experiment was done in 2010 and the results were reported at a seminar, 27 September 2010, FLNP JINR, Dubna, Russia and at the Conference on neutron reflectometry SUPER ADAM, 25–26 October 2010, Grenoble, France. The initial results were published in [12,13]. The private oral communication [11] was done by Nikitenko in December 2012 after the publication of our preprint [13] and its submission to JETP. The results of this early experiment were not published.

We consider a waveguide structure of the type Fe(10 nm)/Cu(150 nm)/Fe(50 nm)//glass. In such a structure, resonant modes characterized by a quantum number n are excited in the guiding Cu layer for specific incidence angles [2]. Figure 1 shows the propagation of the resonance mode $n = 2$ for a spin-up neutron inside the guiding layer, over the length of 100 μm. The propagation length can be further increased by selecting a lower order mode, by increasing the thickness of the top Fe coupling layer, the thickness of the guiding layer, the potential well depth, or the coherence of the incident beam (decreasing the divergence). This is not shown because the corresponding figures are far less legible. In optimal conditions, it is possible to reach mm size length scales.

A specific geometry can be considered where the resonant mode propagates along the channel and eventually exits the channel edge (Fig. 2). If part of the sample surface above the channel is shielded from the incident wave (Fig. 2), we show that the wave field exponentially decreases along the channel, $\sim \exp(-x/x_e)$, where x_e is the channeling length.

An analytic description of the neutron resonances in layered structures can be found in [14,16]. We consider a neutron plane wave with the wave vector \mathbf{k}_0 incident on the structure in Fig. 2 with a grazing angle α_i . The wave function in the resonant layer can be represented as

$$\psi(r) = A \exp(ik_{0x}x) \times (\exp(-ik_{2z}z) + R_{23} \exp(ik_{2z}z)), \quad (1)$$

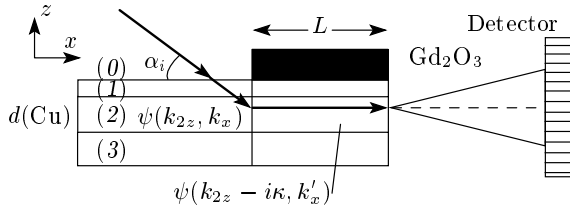


Fig. 2. Experimental setup. The neutron beam enters from the air (0), tunnels through the upper tunneling layer (1) into the channel (2), and is reflected from the reflector layer (3). The waveguide is covered with an absorber of variable length L at its end. The neutron wave is guided inside the channel (2). d is the thickness of the guiding layer (Cu). The neutron wave function in the channel is $\psi(k_{2z}, k_x)$ under the illuminated part of the sample surface and $\psi(k_{2z} - i\kappa, k'_x)$ under the nonilluminated part. k_{2z} is the real part of the component of the wave vector perpendicular to the sample surface, k_x is the real part of the component of the wave vector parallel to the sample surface under the illuminated part, k'_x is the real part of the component of the wave vector parallel to the sample surface under the nonilluminated part, and κ is the imaginary part of the neutron wave vector component perpendicular to the sample surface under the nonilluminated part

where $k_{2z} = \sqrt{k_{0z}^2 - u_{Cu}}$ is the z -component of the neutron wave vector inside the guiding Cu layer, u_{Cu} is the optical potential of the Cu layer, R_{23} is the reflection amplitude from the bottom Fe barrier (3) within the Cu layer (2), and the point $z = 0$ coincides with the interface of the bottom Fe layer. The factor A is the amplitude of the wave incident on the bottom Fe layer. It is determined from the self-consistent equation [16]

$$A = T_{02} \exp(ik_2d) + R_{21}R_{23} \exp(2ik_2d) A, \quad (2)$$

where T_{02} is the transmission amplitude through the top Fe barrier from the vacuum (0) to the Cu layer (2), and R_{21} is the reflection amplitude within Cu (2) from the top Fe barrier (1). It follows from (2) that

$$|A| = \frac{|T_{02}|}{|1 - R_{21}R_{23} \exp(2ik_2d)|}, \quad (3)$$

and hence A has maxima at resonances $k_{0z} = k_0 \sin \alpha_n$, satisfying the equation

$$\gamma(k_{0z}) = 2k_{2z}d + \arg(R_{21}) + \arg(R_{23}) = 2\pi n. \quad (4)$$

The neutron wave function under the nonilluminated section of the waveguide can be represented as the product $Z(z)X(x)$, as in (1). The $Z(z)$ part,

$$Z(z) = A (\exp(-ik'_{2z}z) + R_{23} \exp(ik'_{2z}z)), \quad (5)$$

should not change along the channel, and $X(x) = \exp(ik'_x x)$. The amplitude A in (5) should be the same as in the illuminated part, but k_{2z} should acquire a negative imaginary part $k'_{2z} = k_{2z} - i\kappa$ in the nonilluminated part of the channel. Without this imaginary part, the function $Z(z)$ cannot stay the same in the shadowed region. Indeed, the wave $\exp(-ik'_{2z}z)$ after reflection from the bottom layer, propagation to the top layer, and coming back to the bottom layer acquires the amplitude $R_{23}R_{21} \exp(2ik'_{2z}d)$. If we want this amplitude to remain unity as at the start, we must have

$$R_{23}R_{21} \exp(2ik'_{2z}d) = 1.$$

Whence it follows that the real part of k'_{2z} is equal to k_{2z} to satisfy resonance condition (4), the imaginary part should be $\kappa = -\ln |R_{21}R_{23}|/2d$ to compensate the losses because of transmissions through both Fe layers. If the thicknesses of the two Fe layers in Fig. 1 are large enough, then $|R_{21}R_{23}| \approx 1$ and κ is small.

To find the propagation wave vector k'_z in the channel under the nonilluminated area, we use the energy conservation law

$$(k_{2z} - i\kappa)^2 + k'^2_x = k_{2z}^2 + k_x^2, \quad (6)$$

from which it follows that

$$k'_x = \sqrt{k_x^2 + 2i\kappa k_{2z}} \approx k_x + i\kappa k_{2z}/k_x. \quad (7)$$

The imaginary part of k'_x is positive, which leads to

$$X(x) = \exp(ik'_x x) = \exp\left(ik_x x - \frac{x}{2x_e}\right)$$

and thus to the exponential decay of the intensity $I \propto \exp(-x/x_e)$ with the channeling length

$$x_e = \frac{k_x}{2\kappa k_{2z}} \approx \frac{k_x d}{k_{2z} |\ln |R_{21}R_{23}||}. \quad (8)$$

The investigated waveguide structure was Fe(200 Å)/Cu(1400 Å)/Fe(500 Å)//glass(substrate) with magnetically saturated Fe layers. This system in the case of a fully magnetized Fe state represents a potential well between two high potential barriers for neutrons polarized parallel to the Fe magnetization. Inside the guiding layer, the neutron wave function at the resonance $n = 0$ has the amplitude $A = 17.1$, comparable to unity of the incident wave amplitude. In what follows, we discuss our results on neutron channeling at the resonance $n = 0$, which is characterized by the highest neutron wave function amplitude.

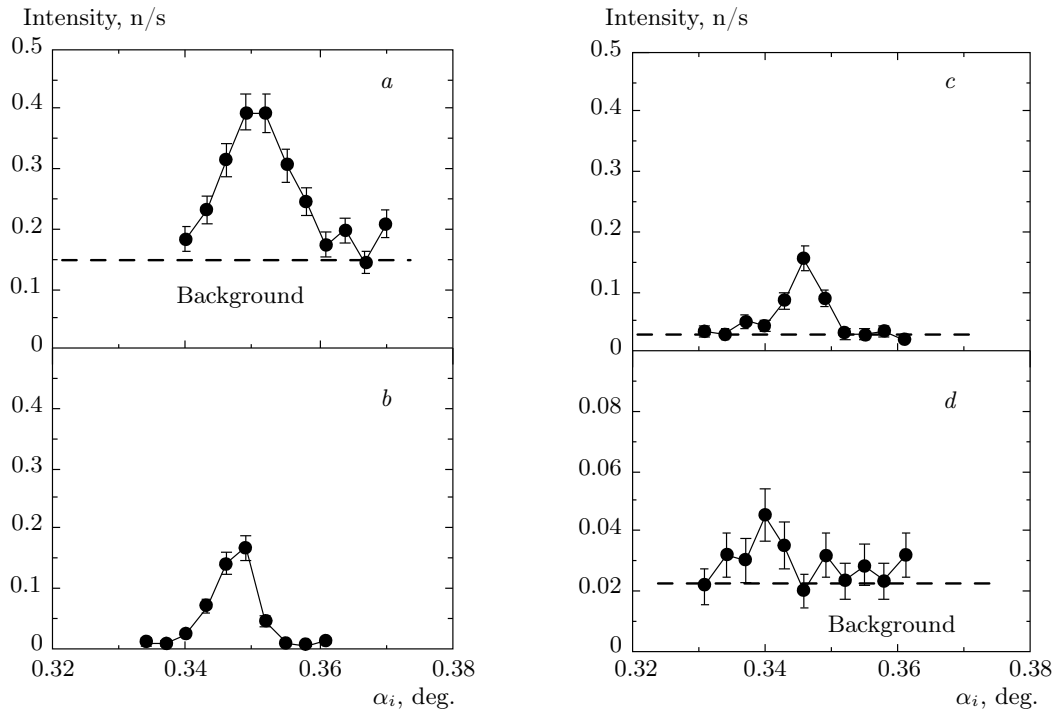


Fig. 3. Neutron microbeam intensity as a function of the incidence angle α_i for different lengths of the absorbing Gd_2O_3 powder layer (see Fig. 2). The incidence angle scales are slightly shifted with respect to each other because the sample was remounted for each measurement. The dashed line marks the background level. $L = 0$ (a), 2 (b), 4 (c), 6 (d) mm

The experiment was carried out at the polarized neutron reflectometer N-REX⁺ (Forschungsneutronenquelle Heinz Maier-Leibnitz, FRM II, Garching, Germany) with the surface of the waveguide sample oriented horizontally. The neutron wavelength was 4.26 Å (FWHM = 1%), the incidence angle resolution was 0.006°. Magnetized supermirrors in transmission mode were used as the neutron spin polarizer and analyzer. The polarization of the incident beam was 97% and the polarizing efficiency of the analyzer was 94%. A Mezei-type spin-flipper of 100% efficiency was used to flip the polarization of the incident beam. The reflectivity of the waveguide structure was measured using a two-dimensional position-sensitive ³He gas detector with a spatial resolution of 3 mm (FWHM). The distance between the collimating diaphragm and the waveguide sample was 2200 mm, the sample-detector distance was 2500 mm. As an absorber, we used Gd_2O_3 powder with a grain size of about 1 μm, such that the optical properties of the waveguide not be altered by the absorber. The height of the applied Gd_2O_3 powder was 2–3 mm, which was sufficient to absorb the reflected beam. The dry powder was carefully put by hand onto the sample surface according to the desired length L of the coverage.

The sample size was 30 × 30 × 5 mm³. The sample structure determined from specular reflectivity [4] was $\text{FeO}(54 \text{ \AA})/\text{Fe}(154 \text{ \AA})/\text{Cu}(1360 \text{ \AA})/\text{Fe}(510 \text{ \AA})/\text{glass}$ (substrate). A waveguide resonance was experimentally found in [4] at the incidence angle $\alpha_0 = 0.37^\circ$, which is in good agreement with theoretical values following from Eq. (5): $\alpha_0 = 0.365^\circ$.

The neutron microbeam intensity measured for the up polarization of the incident beam near the resonance $n = 0$ is shown in Fig. 3 as a function of the incidence angle α_i for different absorber lengths L . This microbeam intensity was determined by integration over a narrow interval of outgoing angles ($\pm 0.1^\circ$) around the sample horizon, which was defined by the analyzer aperture. The microbeam intensity without any absorber coverage ($L = 0$) is accompanied by a high level of background arising from the specularly reflected beam. The background level for practically any minute length of the absorber coverage is much lower due to the blocking of the reflected beam by the macroscopic barrier of Gd_2O_3 powder.

The angular positions of the peaks in the microbeam intensity shown in the four panels of Fig. 3 are not exactly identical due to slightly different ex-

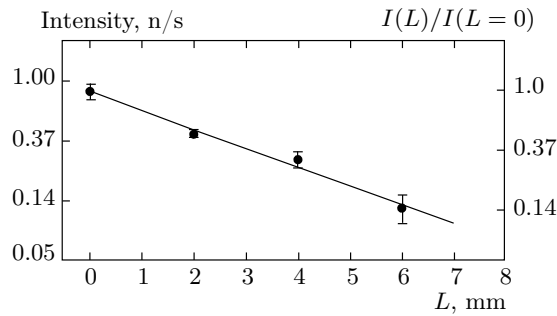


Fig. 4. Microbeam intensity (after the background subtraction) as a function of the absorber length L in the natural logarithmic ordinate scale

perimental offsets in the incidence angles scales. The sample was removed and placed back after each measurement to change the absorber length. After that, the angular offset was not checked and revised because the specularly reflected beam was blocked by the absorber. For the purpose of this article, however, the absolute peak positions are not needed.

The integrated peak area $I(x)$ of the microbeam intensities displayed in Fig. 3 is plotted as a function of the absorber length L in Fig. 4 with logarithmic ordinate scales. The left ordinate axis represents absolute neutron intensities after the background subtraction, with the background level defined by the intensity outside the resonance (marked by dashed lines in Fig. 3). The right ordinate axis represents neutron intensities relative to the intensity without the absorber ($L = 0$). An exponential fit to the data yields $x_e = (3.2 \pm 0.3)$ mm for the neutron channeling length, with the error margin estimated from the statistical experimental errors. This result is in good agreement with the theoretical value 3.14 mm obtained from Eq. (8). This good agreement shows that our waveguide is of very good quality. Other than tunneling through the upper coupling layer loss mechanisms, scattering losses due to interface roughness or bulk inhomogeneities turn out to be negligible for the investigated waveguide.

Our results show that it is possible to efficiently couple a beam of the width $x_e \sin \alpha_0 \approx 20 \mu\text{m}$ into the waveguide and to carry it to the edge of the guiding layer of thickness 1400 Å. This corresponds to a spatial compression ratio higher than 100 (in one direction). Compared to other focusing systems providing also very high compression ratios (such as compound refractive lenses [1]), the layered planar waveguide discussed here has the advantage of producing a very clean

microbeam. The use of a planar waveguide allows effectively extracting a microbeam from the direct and reflected beams. Using absorbers, a better signal-to-noise ratio can be obtained (cf. Fig. 3a and Fig. 3b).

Polarized neutron microbeams could be practically used for the investigation of magnetic nanostructures with high spatial resolution in one dimension. In particular, this opens up possibilities for the study of magnetic microstructures either by direct precession techniques [17–19] or by phase imaging [20]. Resonant beam couplers may also be used for the production of very high resolution long wavelengths monochromators [21].

In conclusion, we have reported the experimental determination of the neutron channeling length in a planar waveguide structure. The intensity of the neutron microbeam emerging from the edge of the waveguide was recorded as a function of the absorber length at the waveguide surface, which defines the nonilluminated area. The observed decay length agrees well with the theoretical prediction in (8). This knowledge should allow optimizing neutron waveguide structures.

We furthermore expect that the described method to determine the channeling length can be used to characterize imperfections in waveguides via the associated decrease in the channeling length. This experimental method can thus contribute to the further development of the theory of channeling in waveguides and to the development of optimized devices for the production of neutron microbeams for the characterization of nanostructures. The method may also more generally prove to be useful as a sensitive tool to characterize chemical, structural, and magnetic imperfections in thin layered structures.

The authors are thankful to T. Keller for the discussions and J. Franke for the technical help during the experiments. The support of the management and staff at FRM II, Garching, is gratefully acknowledged. This work has been supported by a Focused Neutron Research Funding of the Max Planck Society, Munich. Partially this work has been supported by the French project IMAMINE 2010-09T.

REFERENCES

1. F. Ott, in: *Modern Developments in X-Ray and Neutron Optics*, Springer Series in Optical Sciences (2008), Vol. 137, p. 113.
2. F. Pfeiffer, V. Leiner, P. Høghøj, and I. Anderson, *Phys. Rev. Lett.* **88**, 055507 (2002).

3. F. Pfeiffer, P. Hoghoj, I. S. Anderson, and V. Leiner, Proc. SPIE **4509**, 79 (2001).
4. S. V. Kozhevnikov, A. Rühm, F. Ott et al., Physica B **406**, 2463 (2011).
5. S. V. Kozhevnikov, A. Rühm, and J. Major, Crystallogr. Rep. **56**, 1207 (2011).
6. Y. P. Feng, C. F. Majkrzak, S. K. Sinha et al., Phys. Rev. B **49**, 10814 (1994).
7. S. P. Pogossian, A. Menelle, H. Le Gall et al., Phys. Rev. B **53**, 14359 (1996).
8. A. Menelle, S. P. Pogossian, H. Le Gall et al., Physica B **234-236**, 510 (1997).
9. V. L. Aksenov, Yu. V. Nikitenko, A. V. Petrenko et al., FLNP Annual report 2000, Dubna (2001), p. 239.
10. V. L. Aksenov and Yu. V. Nikitenko, Physica B **297**, 101 (2001).
11. Yu. V. Nikitenko, *Measurement of the Neutron Channeling Length in Waveguides*, private communication (2012).
12. S. V. Kozhevnikov, F. Ott, A. Rühm, and J. Major, FLNP Annual Report 2011, ed. by A. V. Belushkin and O. A. Culicov (2012); http://flnp.jinr.ru/img/572/1097_10_experimental_reports_2011.pdf.
13. S. V. Kozhevnikov, V. K. Ignatovich, F. Ott, A. Rühm, and J. Major, Preprint JINR E14-2012-117 (2012).
14. V. K. Ignatovich and F. Radu, Phys. Rev. B **64**, 205408 (2001).
15. V. O. de Haan, J. Plomp, T. M. Rekveldt et al., Phys. Rev. Lett. **104**, 010401 (2010); V. K. Ignatovich, Phys. Rev. Lett. **105**, 018901 (2010).
16. F. Radu and V. K. Ignatovich, Physica B **292**, 160 (2000).
17. P. Thibaudeau, F. Ott, A. Thiaville et al., Europhys. Lett. **93**, 3700 (2011).
18. S. V. Kozhevnikov, T. Keller, Yu. N. Khaydukov et al., arXiv:1209.3889; <http://arxiv.org/abs/1209.3889>.
19. S. V. Kozhevnikov, F. Ott, J. Torrejón, M. Vázquez, and A. Thiaville, Preprint JINR P14-2012-116 (2012), in rus. Submitted to Fizika Tverd. Tela (Phys. Sol. St.).
20. S. P. Krüger, H. Neubauer, M. Bartels et al., J. Synchrotron Radiation **19**, 227 (2012).
21. Y. P. Feng, S. K. Sinha, H. W. Deckman et al., Phys. Rev. Lett. **71**, 537 (1993).